Title

Differing intrinsic biological properties between forebrain and spinal oligodendroglial lineage cells.

Journal

Journal of neurochemistry, 142(3)

ISSN

0022-3042

Authors

Horiuchi, Makoto
Suzuki-Horiuchi, Yoko
Akiyama, Tasuku
et al.

Publication Date

2017-08-01

DOI

10.1111/jnc.14074

Peer reviewed

HHS Public Access

Author manuscript

J Neurochem. Author manuscript; available in PMC 2019 March 16.

Published in final edited form as:

J Neurochem. 2017 August ; 142(3): 378–391. doi:10.1111/jnc.14074.

Differing intrinsic biological properties between forebrain and spinal oligodendroglial lineage cells

Makoto Horiuchi[1], **Yoko Suzuki-Horiuchi**[2], **Tasuku Akiyama**[3], **Aki Itoh**[4,5], **David Pleasure**[4,5], **Earl Carstens**[6], and **Takayuki Itoh**[4,5]

[1]Shriners Hospitals Pediatric Research Center, Temple University School of Medicine, 3500 North Broad Street, Philadelphia, Pennsylvania 19140.

[2]Department of Dermatology, Institute of Regenerative Medicine, University of Pennsylvania School of Medicine, Philadelphia, Pennsylvania, 19104.

[3]Temple Itch Center, Department of Dermatology, Department of Anatomy and Cell Biology, Temple University School of Medicine, 3500 North Broad Street, Philadelphia, Pennsylvania 19140.

[4]Institute for Pediatric Regenerative Medicine, Shriners Hospitals for Children Northern California, 2425 Stockton Boulevard, Sacramento, California 95817.

[5]Department of Neurology, School of Medicine, University of California, Davis, 4860 Y Street, Suite 3700, Sacramento, California 95817.

[6]Department of Neurobiology, Physiology & Behavior, University of California, Davis, 1 Shields Avenue, Davis, California 95616.

Abstract

Differentiation of oligodendroglial progenitor cells (OPCs) into myelinating oligodendrocytes is known to be regulated by the microenvironment where they differentiate. However, current research has not verified whether or not oligodendroglial lineage cells (OLCs) derived from different anatomical regions of the central nervous system (CNS) respond to microenvironmental cues in the same manner. Here, we isolated pure OPCs from rat neonatal forebrain (FB) and spinal cord (SC) and compared their phenotypes in the same *in vitro* conditions. We found that although FB and SC OLCs responded differently to the same external factors; they responded differently to proliferation to mitogens, oligodendrocyte phenotype after differentiation, and cytotoxic responses to α-amino-3-hydroxy-5-methyl-4-isoxazolepropionate-type glutamate receptor-mediated excitotoxicity at immature stages of differentiation in a cell-intrinsic manner. Moreover, transcriptome analysis identified genes differentially expressed between these OPC populations, including those encoding transcription factors (TFs), cell surface molecules, and signaling molecules. Particularly, FB and SC OPCs retained the expression of FB- or SC-specific TFs, such as Foxg1 and Hoxc8, respectively, even after serial passaging *in vitro*. Given the essential role of these TFs in the regional identities of CNS cells along the rostrocaudal axis, our results suggest

Address correspondence to Makoto Horiuchi, Ph.D., Shriners Hospitals Pediatric Research Center, Temple University School of Medicine, 3500 North Broad Street, MERB, Rm: 681, Philadelphia, Pennsylvania 19140, Phone: (215) 926-9334; makoto.horiuchi@temple.edu.

that CNS region-specific gene regulation by these TFs may cause cell-intrinsic differences in cellular responses between FB and SC OLCs to extracellular molecules. Further understanding of the regional differences among OPC populations will help to improve treatments for demyelination in different CNS regions and to facilitate the development of stem cell-derived OPCs for cell transplantation therapies for demyelination.

Graphical Abstract

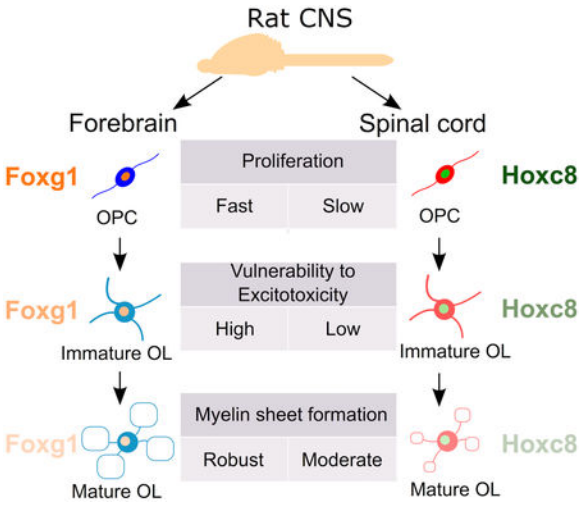

Comparison of oligodendroglial lineage cells (OLCs) isolated from neonatal rat forebrains and spinal cords *in vitro* revealed that these OLCs are cell-intrinsically different in terms of proliferation, susceptibility to excitotoxicity, and myelin sheet formation. Transcriptome analysis demonstrated that OLCs retain region-specific transcription factors of their origin, such as Foxg1 and Hoxc8, suggesting their role in the phenotypic differences of OLCs.

Keywords

Proliferation; Differentiation; Excitotoxicity; Hox gene; Rostrocaudal axis

Introduction

During the development of the mammalian central nervous system (CNS), the differentiation of oligodendroglial progenitor cells (OPCs) into myelinating oligodendrocytes occurs mainly after neurogenesis, astrocytogenesis, and axonal wiring in the CNS. The proliferation and migration of OPCs and their differentiation to oligodendrocytes have been considered to be regulated mainly by external stimuli produced by other cell types in the CNS rather than by OPC-intrinsic mechanisms. A variety of growth factors and neurotrophic factors such as PDGFA homodimer ($PDGF_{AA}$), FGF2, neuregulins, and NT-3, have been identified as factors essential for generation and development of oligodendroglial lineage cells (OLCs) and CNS myelination (Barres & Raff 1994, Miller 2002). In pathological conditions, such as perinatal brain injury, myelination by OPCs is negatively affected by extracellular glutamate and inflammatory cytokines, such as IL-1β and TNFα (Cai et al. 2004, Carty et al. 2011,

Johnston 2005). We previously demonstrated that interferon-γ (IFNγ), a type-I T helper cell-derived cytokine, also induces apoptosis of OPCs suggesting its negative effects on developmental myelination (Horiuchi et al. 2006, Horiuchi et al. 2011). Studies suggest that these factors also affect remyelination in the adult CNS after demyelination occurring in multiple sclerosis and traumatic brain or spinal cord injury (Bannerman et al. 2007, Levine 2016, Lin et al. 2006). Highly purified primary OLC cultures from rodents have provided a useful model to examine the direct effects of these factors on OLCs (Horiuchi et al. 2010). In most studies, OPCs isolated from optic nerves or brains were employed as models representing the OPCs in the entire CNS regions (Barres & Raff 1994, Groves et al. 1993). However, little is known about whether or not OPCs from different CNS regions are the same in terms of the response to these extracellular factors.

OLC heterogeneity in morphology, including variability in number and length of internodes of myelinating oligodendrocytes, has been reported (Weruaga-Prieto et al. 1996). A recent study using single cell RNA sequencing revealed molecular heterogeneity of OLCs in different CNS regions *in vivo* as well (Marques et al. 2016). Several studies have also addressed the heterogeneity in the origins of OPCs. In the forebrain (FB), multiple subpopulations of OPCs are generated from different domains along the dorsoventral (DV) axis of the neural tube at distinct embryonic ages, and these subpopulations compete for space in the developing FB (Kessaris et al. 2006). In the spinal cord (SC), there are two waves of OPC generation; the first wave occurs around embryonic day 12.5 (E12.5) from the ventral midline at, and then the second wave of OPCs is generated from the lateral and dorsal plates. These two populations show distinct preferences in axonal tracts they myelinate (Tripathi et al. 2011). Phenotypic differences between white and gray matter OPCs have also been reported. Hill and his colleagues, using organotypic slice cultures, demonstrated that OPCs in neonatal mouse white and gray matter differ in their proliferative response to $PDGF_{AA}$ due to OPC-intrinsic mechanisms (Hill et al. 2013). A study using a transplantation strategy demonstrated that adult OPCs from cortical white matter differentiate into myelinating oligodendrocytes more efficiently than those isolated from gray matter in either white or gray matter of the host CNS (Vigano et al. 2013).

In the developing neural tube, rostrocaudal (RC) patterning precedes DV patterning. This was demonstrated by the removal of hedgehog signaling from the neural tube after the establishment of RC patterning that was sufficient to inhibit DV patterning (Fuccillo et al. 2004). Compared with the OPC heterogeneities along the DV axis, regional differences of OPC populations at different RC levels are not yet well understood. Recently, Bechler et al. (2015) have shown that rat oligodendrocytes purified from SC formed longer internodes on microfibers than those from the cortex *in vitro;* demonstrating that oligodendrocytes from different RC regions generate sheath lengths. But, the molecular basis of the OLCs regional identity is not yet understood. CNS region-specific transcription factors (TFs), such as Hox TFs, expressed in a spatially restricted manner along the RC axis, are considered as determinants of the positional identity of neuroepithelial precursor cells and their progenies along the RC axis. The Nazarali laboratory reported the expression of Hox TFs in cerebral cortex-derived oligodendrocytes in mixed glial cultures (Nicolay et al. 2004, Booth et al. 2007). Miguez and colleagues demonstrated the expression of Hox2a and Hox2b in $Olig2^{+}$ progenitor cells in the fetal hindbrain and revealed their roles in oligodendrogenesis (Miguez

et al. 2012). It has been reported that neural stem cells (NSCs) retain region-specific Hox gene expression during multiple *in vitro* expansion, while they maintain NSCs properties. This indicates that the RC patterning information is maintained in NSCs by a cell autonomous mechanism (Kelly et al. 2009). However, it is not well understood how the expression of Hox TFs is regulated in OPCs. Furthermore, little is known about differences in intrinsic biological properties among OPCs derived from different RC levels, except for the sheath length.

In this study, we directly compared highly purified primary rat OPCs cultures from the FB and the SC, two different RC compartments of the CNS, maintained under identical culture conditions. OPCs purified from the neonatal rat FB have been well characterized by us and others (Mayer-Proschel 2001, Horiuchi et al. 2006, Horiuchi et al. 2010). SC OPCs were purified and expanded by exactly the same method and compared with the FB OPCs in terms of 1) proliferation response to external factors, 2) phenotypic changes after induction of oligodendroglial differentiation, 3) vulnerability to α-amino-3-hydroxy-5-methyl-4-isoxazolepropionate-type glutamate receptor (AMPAR)-mediated excitotoxicity and to IFNγ-induced cytotoxic effects, and 4) comprehensive gene expression profile. We found that SC OLCs are substantially different from their FB counterparts in these biological properties in a cell-intrinsic manner.

Materials and Methods

Reagents and chemicals

All reagents, including anti-2',3'-cyclic nucleotide-3'-phosphodiesterase (CNP) antibody (RRID:AB_476854), and culture media used in this study were purchased from SIGMA-Aldrich (St. Louis, MO) and Thermo Fisher (Carlsbad, CA), respectively, except for the following products: Human recombinant FGF2, $PDGF_{AA}$, and rat recombinant IFNγ were from R&D systems (Minneapolis, MN). Rat anti-myelin basic protein (MBP, RRID:AB_531559) and rabbit anti-myelin proteolipid protein (PLP, RRID:AB_11026674) antibodies were from Novus (Littleton, CO). Mouse and rabbit anti-β-actin antibodies (RRID:AB_2242334 and AB_1903890, respectively) were from Cell Signaling Technology (Danvers, MA). Mouse anti-myelin oligodendrocyte glycoprotein (MOG, RRID:AB_1587278), and rabbit-anti-NG2 chondroitin sulfate proteoglycan (NG2, RRID:AB_476854), anti-GRIA2 (RRID:AB_2113875), anti-GRIA2/3 (RRID:AB_310741), and anti-GRIA4 (RRID:AB_90711) antibodies were from Millipore (Billerica, MA). RIDye 800CW-conjugated and RIDy 680RD-conjugated secondary antibodies (RRIDs:AB_10793856, AB_10796098, AB_621840, AB_621841, & AB_1850025) for Western blotting were from LI-COR (Lincoln, NE). 5-ethynyl-2′-deoxyuridine (EdU), pacific blue-conjugated azide, fura-2 acetoxymethyl ester (AM) (RRID:AB_11156243), and pluronic F-127 were from Thermo Fisher.

Mixed glial culture

Rat primary mixed glial cultures were prepared as described previously (Horiuchi et al. 2006). Briefly, FBs and whole SCs were dissected from postnatal day 0-2 (P0-2) or E14 Sprague-Dawley rats (RRID:RGD_5508397, Charles River, Wilmington, MA) and EGFP-

transgenic Lewis rats (Lew-Tg(CAG-EGFP)YsRrrc)(RRID:RGD_6478789, Rat Research and Resource Center, Columbia, MO). After cleaning off meninges and vessels, the remaining tissue was cut into small chunks with a 21-gauge needle and digested by 0.0625% (w/v) trypsin in Ca^{2+} and Mg^{2+}-free Hank's balanced salt solution (HBSS) for 20 min. Dissociated cells were obtained by passing the softened chunks through a 1 ml pipette tip several times, and collected by centrifugation at 365 xg for 5 min. The cells were resuspended in minimum essential medium alpha containing 5% (v/v) fetal bovine serum and 5% (v/v) calf serum and plated onto a 10 cm culture dish. One day after plating, attached cells (designated as passage 0) were washed with HBSS to remove serum, and thereafter maintained in the growth medium, a 3:7 mixture (v/v) of B104 neuroblastoma (RRID:CVCL_0154)-conditioned medium and the N1 medium (high glucose Dulbecco's modified Eagle's medium supplemented with 6 mM $_{L}$-glutamine, 10 ng/ml biotin, 5 μg/ml insulin, 50 μg/ml apo-transferrin, 30 nM sodium selenite, 20 nM progesterone and 100 μM putrescine as final concentrations). Cultures were fed with fresh growth medium every other day for 5 days. Both sexes were used for cell cultures. The University of California Davis Institutional Animal Care and Use Committee approved all animal experiments.

Purification of A2B5+ rat OPCs by immunopanning

Mixed glial cultures were washed with HBSS, suspended in the N1 medium containing 0.1% (w/v) BSA, and plated and incubated on negative immunopanning plates coated with RAN-2 (RRID:CVCL_G149) antibody for 30 min at 37°C to exclude RAN-2-positive cells. Following two rounds of this negative selection, nonadherent cells were transferred to positive panning plates coated with A2B5 antibody (RRID:CVCL_7946). After 30 min incubation, the positive panning plates were washed with HBSS three times to remove A2B5-negative cells. A2B5+ cells were collected from the plates by trypsinization. Purified cultures were expanded up to passage 4 in growth medium supplemented with 5 ng/ml human recombinant FGF2 and 1 ng/ml human recombinant $PDGF_{AA}$. OPCs were fed with fresh growth medium every other day. At least three OPC cultures were prepared independently from each of the P0-2 forebrain, the P0-2 spinal cord, and the E14 spinal cord, and used for all experiments in this study to confirm the reproducibility of data unless otherwise mentioned. To induce *in vitro* differentiation of OPCs into oligodendrocytes, culture medium was switched from growth medium to differentiation medium, a 1:1 mixture (v/v) of high glucose Dulbecco's modified Eagle's medium and Ham's F-12 medium supplemented with 4.5 mM $_{L}$-glutamine, 10 ng/ml biotin, 12.5 μg/ml insulin, 50 μg/ml transferrin, 24 nM sodium selenite, 10 nM progesterone, 67 μM putrescine, and 0.4 μg/ml 3,5,3',5'-tetraiodothyronine as final concentrations. We designated the OLCs at 2 and 4 days in differentiation medium as immature oligodendrocytes (IM) and mature oligodendrocytes (MO), respectively, depending on the expression of differentiation markers in the majority of the cells (Horiuchi et al. 2006).

Immunocytochemistry

Cells cultured on poly-$_{D}$-lysine-coated coverslips were incubated with primary antibodies against cell surface antigens, such as A2B5, O4 (RRID:CVCL_Z932), and H8H9 hybridoma supernatants (undiluted), and anti-NG2 antibody (1:50), at room temperature for 30 min. After washing with PBS, cells were fixed with 4% paraformaldehyde at room temperature

for 15 min and then permeabilized with 100% methanol at −20°C for 15 min. Incubation with anti-MBP antibody (1:10) was performed at room temperature for 30 min after permeabilization. After incubation with fluorophore-conjugated secondary antibodies (1:50) at room temperature for 30 min, nuclei were counterstained with 4,6-diamidio-2-phenylindole (DAPI) (0.5 μg/ml) for 10 min, and then the coverslips were mounted on a slide glass with VectorShield (Vector laboratory, Burlingame, CA).

Semi-quantitative RT-PCR

Total RNA was isolated by RNeasy RNA extraction kit (Qiagen, Valencia, CA). RT reaction and semi-quantitative PCR were performed as reported previously (Horiuchi et al. 2006). The following primer sets were used in this study; rat Hoxc8, forward: CCTCCGCCAACACTAACAGT, reverse: GGGGAAGGCCAAAGGTAATA; rat Lhx2, forward: CCAAGGACTTGAAGCAGCTC, reverse: AGGCGAGATCCTAAAACGTG; rat Foxg1, forward: TCAATGACTTCGCAGACCAG, reverse: ATTCTCCCACATTGCACCTC; rat Gapdh, forward: ATTGTCAGCAATGCATCCTGCA, reverse: AGACAACCTGGTCCTCAGTGTA. Small variability among RT products was verified by semi-quantitative PCR for Gapdh. To confirm reproducibility of the results, each RT-PCR was repeated twice using total RNA samples from at least two independently prepared cultures.

5-Ethynyl-2’-deoxyuridine (EdU)-incorporation assay

Cell cycling rate was measured by EdU-incorporation assay as described previously (Horiuchi et al. 2012b). Briefly, cells were incubated with 10 μM EdU for 4 h. Then, trypsinized cells were collected and fixed with ice-cold 70% (v/v) ethanol. EdU was detected using a pacific blue-conjugated azide according to the manufacturer’s instruction. Samples were acquired by Cyan-ADP flow cytometry (Dako cytomation, Carpinteria, CA), and the number of EdU-positive cells in either EGFP-positive or negative cell population was separately counted by gating with Summit software (Dako cytomation). The cell cycle time (Ct) of FB OPCs was accurately determined as 19 ± 2 h (n=9 wells) by the combination of 5-bromo-2’-deoxyuridine and propidium iodide in our previous study (Horiuchi et al. 2006). Given that EdU incorporation negatively correlates to Ct, the Ct of SC OPCs was estimated as 19 times the reverse of the ratio of EdU+ cell percent in SC cultures to that in FB cultures.

Western blotting

Protein lysates were prepared in the lysis buffer as described previously (Horiuchi et al. 2006). Twenty μg of protein from each sample was size-fractioned by SDS-polyacrylamide gel electrophoresis, transferred onto a nitrocellulose membrane (Schleicher & Schnell, Keene, NH), and probed with primary antibodies for MBP (1:1000), PLP (1:1000), CNP (1:500), MOG (1:1000), and β-actin (ACTB) (1:1000) at 4°C for overnight. For GRIA2, GRIA2/3, and GRIA4, fifty μg of protein from each sample was used. Membranes were incubated with primary antibodies against GRIA2 (1:500), GRIA2/3 (1:500), and GRIA4 (1:500) for 2h at room temperature. Full range recombinant Rainbow Molecular Weight Marker (Amersham Biosciences, Piscataway, NJ) was used as a reference for molecular sizes. IRDye 800CW- or IRDye 680RD-conjugated goat antibodies were used as secondary

antibodies. Immunoreactive signals were detected by Odyssey CLx infrared scanning system (LI-COR). ACTB blotting was used as a loading reference for normalization of proteins of interest using LI-COR Image Studio software (LI-COR).

3-(4,5-Dimethylthiazol-2-yl)-2,5-diphenyltetrazolium bromide (MTT) Assay

Cell viability was estimated by the enzymatic conversion of MTT to formazan crystals in live cells as described previously (Horiuchi et al. 2006). Formazan was dissolved in dimethyl sulfoxide at 90 min after addition of MTT (0.5 mg/ml) to the culture medium, and quantified by a spectrophotometer or a microplate reader at 560 nm.

Time-lapse imaging

Cell death was assessed by time-lapse imaging employing the Nikon Perfect Focus System (Nikon, Tokyo, Japan) with an environmental chamber as described previously (Horiuchi et al. 2010). Serial phase contrast images of each selected field within each well were taken at 5 min intervals for 24 h. 30 cells per field were randomly selected and tracked in the serial images. Cell death was identified by the shrinkage of cell body and processes followed by the cessation of cellular movements as indicated by arrows in Figure 5D.

Calcium imaging

Intracellular free Ca^{2+} concentration, $[Ca^{2+}]_{I,}$ was quantified by microfluorometry with fura-2 AM, as previously described (Akiyama et al. 2014, Itoh et al. 2002). Briefly, OLCs grown on poly-$_D$-lysine-coated coverslips were incubated for 1 h with 10 μM fura-2 AM and 0.02% pluronic F-127 in standard recording medium (SRM; 140 mM NaCl, 5.4 mM KCl, 1.8 mM $CaCl_2$, 0.8 mM $MgCl_2$, 0.8 mM Na_2HPO_4, 10 mM HEPES, 25 mM $_D$-glucose, pH 7.4). The coverslip was placed in a perfusion chamber (RC-21B; Warner Instrument, Hamden, CT), and residual fura-2 AM in the chamber was washed out with SRM. Intracellular Fura-2 was excited by UV light at 340 nm and 380 nm, alternately, and the emission was collected via a CoolSnap camera attached to a Lambda LS lamp and a Lambda optical filter changer (Sutter Instrument, Cranberry Novato, CA). Ratiometric measurements were made using Simple PCI software (Compix, Cranberry Township, PA) every 15 sec. Cells were perfused with 0.3 mM kainate (KA) at 3 min, washed with SRM at 8 min, and then exposed to 10 μM ionomycin to determine the maximum fluorescence ratio in each cell for normalization.

Transcriptome analysis

Transcriptome analysis was performed with GeneChip Rat Gene 2.0 ST arrays (Affymetrix, Santa Clara, CA). Total RNA samples were reverse-transcribed, amplified, biotinylated, and fragmented using GeneChip WT terminal labeling kit (Affymetrix). Hybridization and scanning were performed at the Microarray core facility, the University of California, Davis. Scanned images were analyzed by GeneChip Command Console software and expression values of each probe set were compared with dChip software (Li & Wong 2001). Two independent RNA samples in each experimental group were analyzed. Genes showing a significant difference ($p < 0.05$) between FB and SC OPCs at 2 times or higher by t-test with

dChip software were subjected to the gene ontology (GO) enrichment analysis using DAVID online tool (Huang da et al. 2009).

Statistical analysis

Data are presented as mean ± SD unless otherwise noted. Statistical significance was determined by Student's t-test to compare two groups and two-tailed ANOVA followed by Student-Newman-Keuls *post hoc* test for more than two groups.

Results

A2B5+ cells isolated from postnatal rat spinal cords were OPCs

A2B5+ cells have been considered to be OPCs not only in the rat brain but also in the rat spinal cord (Hall et al. 1996). With the same purification procedure as used for FB A2B5+ cells, we obtained highly pure A2B5+ cells (99 ± 1%) from the SC as pure as those from the FB (99 ± 1%). Like FB A2B5+ cells, SC A2B5+ cells proliferated and maintained A2B5-immunoreactivity in growth medium (Figure 1). To establish the identity of SC A2B5+ cells as OPCs, cells were cultured in differentiation medium for 4 days. At day 2 in differentiation medium, 94 ± 6% of cells differentiated into O4+ immature oligodendrocytes (IMs) as well as FB A2B5+ cells (96 ± 4%), but the number of MBP+ mature oligodendrocytes (MOs) at day 4 was significantly lower (26 ± 10%) in SC A2B5+ cultures than that in FB A2B5+ cells (79 ± 6%) (Figure 2A-D). We found that the density of SC cells at day 4 in differentiation medium was lower than that of FB cells presumably because SC cells proliferated more slowly than FB cells in growth medium (Figure 2G). Since cell density is known to positively regulate the induction of myelin proteins in differentiating oligodendrocytes (Rosenberg et al. 2008), 4-fold more SC A2B5+ cells were plated to induce differentiation at the same culture density as FB A2B5+ cells just prior to changing the medium from growth medium to differentiation medium. With this plating cell density, SC cells reached a comparable live cell density to FB cultures at day 4 based on the density of unfragmented DAPI+ nuclei (Figure 2G). Immunocytochemistry confirmed that they expressed O4 and GalC at day 2 and MBP at day 4 equally to FB cells. This indicates that the degree of oligodendrocyte differentiation of SC cells was comparable to that of FB cells at both time points (Figure 2E-F and Table 1). Western blotting further confirmed the equivalent expression of MBP in the "x4" SC cultures to that in "x1" FB cultures at day 4 in differentiation medium (Figure 2H,I). These results validated that SC A2B5+ cells are comparable to FB A2B5+ cells which have been well characterized as OPCs in previous studies. Therefore, we term FB and SC A2B5+ cells as FB and SC OPCs, respectively, in this study. The x4 plating was used for preparing IMs and MOs from SC OPCs in the all following experiments.

SC OPCs showed a lesser proliferation response to mitogens compared with FB OPCs

As mentioned above, we noticed that, even in the same growth medium, the proliferation of SC OPCs was slower than that of FB OPCs. EdU-incorporation assay showed that, while 55 ± 8% (n=18 wells) of FB OPCs were labeled by EdU after 4 h exposure to EdU in growth medium, 41 ± 5% (n=20 wells) of SC OPCs were labeled ($p<0.01$, Student's t-test) indicating that the cell cycling of SC OPCs was significantly slower compared with FB

OPCs. In rodents, developmental myelination occurs in the SC at late embryonic stages, which is earlier than the post-birth myelination in the FB (Cohen & Guarnieri 1976). This difference in developmental time course between FB and SC OPCs raised the possibility that slow cycling of SC OPCs could be a consequence of their more aged nature compared with FB OPCs at the timing of harvesting (P0-2). To rule out this possibility, SC OPCs were isolated from embryos at E14. EdU-incorporation assay confirmed that the proportion of EdU+ SC OPCs from E14 embryos was not significantly different from that from neonates (42 ± 3%, n=9 wells, vs 41 ± 5%, n=20 wells, respectively, p=0.49, Student's t-test), but was still significantly lower than that of EdU+ FB OPCs from neonates (Figure 3A). Given that the Ct of FB OPCs was measured as 19 ± 2 h (n=9 wells) in our previous study using the same culture model (Horiuchi et al. 2006), the Cts of SC OPCs were estimated as 26 ± 3 h at P0 (n=20 wells) and 25 ± 2 h at E14 (n=9 wells) as described in Materials and Methods.

To examine potential contributions of cell-to-cell interactions such as autocrine mechanisms to their mitotic responses, we prepared mixed culture of FB and SC OPCs in 1:1 ratio, and compared their proliferation by EdU incorporation. To facilitate discrimination between SC and FB OPCs in the mixed cultures, either FB or SC OPCs isolated from wild-type rats were co-cultured with those from EGFP-rats (Figure 3B). As shown in Figure 3C-E, using a flow-cytometer, EGFP− and EGFP+ cells were separated with R2 and R3 gating, respectively, and then the number of EdU+ cells was counted in each of EGFP− and EGFP+ populations. We tested all possible combinations of co-cultures and compared EdU incorporation by each population. We confirmed that the proliferation of FB OPCs was not slowed by co-culturing with SC OPCs and that the proliferation of SC OPCs was not accelerated in the co-culture with FB OPCs (Figure 3F). These results indicate that mitotic responses of these two OPC groups to mitogens were intrinsically different and that there was no paracrine effect between them on the proliferation.

Myelin sheet formation and MOG expression were reduced in differentiated SC MOs compared with FB MOs

Next, we examined differences in differentiation to oligodendrocytes between FB and SC OPCs. For this purpose, four-fold more SC OPCs were plated than FB OPCs to induced *in vitro* differentiation of both cultures at the same cell density. During differentiation, oligodendrocytes form myelin sheets which are MBP+ membrane-like structures filling the space between oligodendroglial processes resembling the myelin membrane *in vivo* (arrows in Figure 4A). We found that SC MOs did not form the typical MBP+ myelin sheets observed in the FB MO cultures (1006 ± 200 μm^2/cell vs 1360 ± 197 μm^2/cell, respectively, Figure 4A-C) despite an equivalent MBP level as shown by Western blots (Figure 4D). SC MOs formed dense MBP+ spots rather than forming MBP+ sheets (Figure 4B). Western blotting showed that MOG expression was significantly lower in SC MOs than in FB MOs, while there was no difference in the expressions of MBP, PLP, or CNP (Figure 4D,E). These results also confirmed phenotypic differences between SC and FB MOs upon *in vitro* differentiation.

SC OLCs showed different vulnerability to KA-induced excitotoxicity from FB OLCs *in vitro*

We previously reported that FB OLCs are vulnerable to KA-induced excitotoxicity and IFNγ depending on their developmental stages; FB OLCs are the most vulnerable to KA at the stage of IM and to IFNγ at the OPC stages, whereas FB MOs are resistant to both factors (Itoh et al. 2002, Horiuchi et al. 2006). To examine whether SC and FB cells are different in cytotoxic responses to these molecules, SC and FB OPCs were plated at x4 and x1 density, respectively, and treated with KA (1 mM) or IFNγ (100 ng/ml) at the three differentiation stages (OPC, IM, and MO). MTT assay at 48 h after treatments showed that FB cells became significantly more susceptible to KA as they differentiate from OPCs to IMs as reported previously (Itoh et al. 2002). However, SC IMs were as susceptible as SC OPCs and significantly more resistant to KA than FB IMs, while SC MOs were slightly but significantly more susceptible to KA than FB MOs (Figure 5A). There were no differences between FB and SC OLCs in the cytotoxic effects of IFNγ (Figure 5B). The dose-response curve to the KA cytotoxicity indicated that SC IMs were significantly more resistant to KA compared with FB IMs at all KA concentrations tested (0.1, 0.3, and 1 mM). We found the greatest difference in survival between FB and SC IMs after a 48 h-exposure to KA at 0.3 mM (Figure 5C). Thus, 0.3 mM KA was used for the subsequent experiments.

Time-lapse observation was conducted with FB and SC IMs treated with 0.3 mM KA to confirm that cell death was reduced in SC IMs compared with FB IMs. Using serial time-lapse images which were taken at 5 min intervals, cell death events were counted (Figure 5D). Cell division was observed in none of the selected cells in FB or SC cultures indicating most of the cells exited the cell cycle at this stage as we reported previously (Horiuchi et al. 2006). This experiment confirmed that the KA-induced cell death was significantly reduced in SC IMs compared with FB IMs, while there was no difference in the basal cell death in the control cultures (Figure 5E).

It is widely accepted that the highest susceptibility of FB IMs to excitotoxicity is attributable to Ca^{2+}-overload through Ca^{2+} permeable AMPARs. OLCs are known to express AMPAR subunits GRIA2, GRIA3, and GRIA4 (Itoh et al. 2002). AMPARs become Ca^{2+} impermeable when at least one edited GRIA2 subunit is present in the heterotetramer of an AMPAR (Sommer et al. 1991, Itoh et al. 2002). Given that virtually 100% of GRIA2s in the CNS and OLCs are edited (Itoh et al. 2002, Kawahara et al. 2003), it is reasonable to assume that Ca^{2+}-permeability of AMPARs inversely correlates with the expression levels of GRIA2. Western blotting using an antibody selective for GRIA2 revealed that the expression level of GRIA2 was significantly higher in SC OLCs than those in FB OLCs at the IM stage (Figure 6A-B) suggesting that SC IMs express more Ca^{2+} impermeable AMPARs than FB IMs.

We also compared $[Ca^{2+}]i$ responses to KA between SC and FB IMs. KA was used at 0.3 mM for Ca^{2+} imaging. However, $[Ca^{2+}]i$ responses of SC IMs during a 5-min exposure to 0.3 mM KA were similar to those of FB IMs in terms of the peak $[Ca^{2+}]i$, the slope during 5 min of KA treatment, and the restoration after washout of KA (Figure 6C,D). There was no significant difference in the averaged $[Ca^{2+}]i$ elevations between FB (53.5 ± 14.6% of the maximum $[Ca^{2+}]i$ induced by 10 μM ionomycin, n=346 cells) and SC IMs (56.5 ± 13.1%, n=280 cells) during the exposure to KA.

FB and SC OPCs expressed different sets of genes including CNS region-specific transcription factors (TFs)

To compare comprehensive gene expression profiles between FB and SC OPCs, microarray analysis was performed using purified OPCs actively growing in growth medium at passage 2. Expressions of the OPC signature genes, Sox10, Olig1/2, Pdgfra, and Cspg4 were similar in both OPC preparations, confirming their identity as OPCs (Figure 7A). Nevertheless, we identified a total of 39 genes which were two-fold or more up-regulated in either FB (16 genes) or SC OPCs (23 genes). Particularly, many CNS region-specific TFs, such as FB-specific Foxg1 and Six3, and SC-specific Hoxc8, Hoxa5, Hoxa6, Hoxa9, and Hoxb8, were expressed in a region-specific manner in FB and SC OPCs (Figure 7B). Non-TF genes were also differentially expressed between FB and SC OPCs to a lesser extent (Figure 7C). Semi-quantitative RT-PCR revealed that another Hox TF, Lhx2, was more highly expressed in FB OPCs than SC OPCs (Figure 7D). Semi-quantitative RT-PCR for Foxg1, Lhx2, and Hoxc8 with FB and SC OPCs at passage 4 (around 3-4 weeks *in vitro*) confirmed that they were continuously expressed in a mutually exclusive manner even after a number of cell divisions under the same culture condition (Figure 7D). These region-specific TFs were down-regulated as OLCs differentiated into IMs and MO *in vitro* (Figure 7E,F). GO enrichment analysis revealed that genes encoding transmembrane proteins, tyrosine kinases, ion channels, and G-protein coupled receptors were enriched in either FB or SC OPCs in addition to Hox TFs (Table 2). These results indicate that, despite their comparable expression profiles of OPC signature genes, FB and SC OPCs differentially express genes involved in multiple aspects of cellular functions including gene transcription, intracellular signal transduction, and ion homeostasis.

Discussion

In this study, we have comprehensively compared OLCs derived from two distinct RC compartments of the CNS, FB and SC, using an *in vitro* paradigm that enabled us to directly compare these two groups under the same experimental conditions. Our data demonstrated that OLCs isolated from neonatal FBs and SCs were cell-intrinsically different in terms of the proliferation response to growth factors, *in vitro* myelin sheet formation, and cytotoxic response to the KA-induced excitotoxicity. Moreover, transcriptome analysis revealed the differential expression of multiple genes between FB and SC OPCs. Among these genes, CNS region-specific TFs corresponding to their anatomical origins were maintained in both OPCs throughout continuous cell divisions *in vitro*. Thus, FB and SC OPCs can be considered as two different OPC lineages with distinct cell-intrinsic biological properties resulted from their regional identities.

Differential proliferation rate between FB and SC OPCs

Proliferation is one of essential features of OPCs and is essential to provide sufficient numbers of oligodendrocytes for complete myelination of axons during development. While mitotic ability of OPCs had been thought to be limited by a cell-intrinsic program known as the “cell-intrinsic timer”, which counts down the number of cell divisions to differentiate into postmitotic oligodendrocytes, subsequent studies demonstrated that OPC proliferation is mainly regulated by extrinsic factors, such as the supply of $PDGF_{AA}$, rather than by a cell-

intrinsic mechanism (Durand et al. 1998, van Heyningen et al. 2001). We found that FB OPCs proliferated at a significantly faster rate than SC OPCs indicating their cell-intrinsic difference in proliferation response to identical culture conditions. The *in vitro* Cts of rat SC OPCs estimated in this study (26 ± 3 h at P0 and 25 ± 2 h at E14) were quite comparable to that of E17 mouse SC OPCs treated with $PDGF_{AA}$ *in vitro* (28 ± 5 h) reported by van Heyningen and his colleagues (van Heyningen et al. 2001). Young and her colleagues showed that the Ct of adult OPCs *in vivo* was significantly shorter in white matter than in gray matter in both FB and SC. Interestingly, they also showed that adult OPCs in the corpus callosum proliferated faster than those in the spinal white matter *in vivo* (Young et al. 2013). Although little is known about environmental factors regulating the Ct of adult OPCs, the *in vivo* proliferation rate of adult white matter OPCs may reflect the cell-intrinsic regional differences of OPCs. Transcriptome analysis identified cell surface receptors differentially expressed by FB and SC OPCs, such as Ednrb, Ephrin receptors, and Lgrs. Given the involvement of these cell surface receptors in the regulation of cell proliferation in glioma and other cell types (Fukai et al. 2008, Carmon et al. 2011, Xie et al. 2016), such a difference in receptor expressions could contribute to the differential proliferation rates between FB and SC OPCs. SC OPCs may require additional mitogens, which are not sufficiently present in growth medium, to stimulate them to proliferate as fast as FB OPCs.

Phenotypic differences between FB and SC MOs

Our data also demonstrate that differentiated FB and SC oligodendrocytes are phenotypically different in terms of myelin sheet formation and MOG expression. Myelin sheets are cholesterol-rich membrane structures resembling compacted myelin sheaths *in vivo*, and their formation has been well studied in axon-free cultures (Aggarwal et al. 2011, Horiuchi et al. 2012a). Previous studies demonstrated that proper interactions between cell surface receptors expressed by differentiating oligodendrocytes and ligands on the extracellular substrate are required for the myelin sheet formation. A variety of receptor-ligand combinations, such as laminin-integrin and ephrin-ephrin receptor, are known to be involved in this process (Chun et al. 2003, Olsen & Ffrench-Constant 2005, Linneberg et al. 2015). As many cell surface receptors are differentially expressed between FB and SC cells at the OPC stage, it is likely that differentiating FB and SC oligodendrocytes also express different cell surface molecules involved in myelin sheet formation. In the MO stage, MOG expression was reduced in SC cultures compared to those with FB cultures. MOG is also a cell surface molecule and suggested to act as a cell adhesion molecule and a regulator of microtubule stability (Johns & Bernard 1999). Such a difference in the expression of cell surface molecules may modulate oligodendrocyte-axon interaction during developmental myelination in the different CNS regions *in vivo* as well. The robustness of myelin sheet formation is also dependent on lipid synthesis during oligodendrocyte differentiation (Maier et al. 2009, Schoenfeld et al. 2010). Thus, it is also possible that the different efficiencies of lipid synthesis between FB and SC OLCs cause the differential myelin sheet formation. *In vivo*, the average internode length is greater in SC than in FB. Recently, Bechler et al. (2015) reported that this difference was reproduced in 3D cultures of purified rat OLCs from the cortex and SC. SC OLCs appeared to mature and form myelin sheaths as well as cortical OLCs in their study, while SC OLCs failed to completely mature in our model. Several differences in culture conditions for mixed glial cultures, methods for OPC purification

(shaking-off vs immunopanning), and OPC density for myelination cultures may have accounted for the differential maturation of SC OLCs between these two studies. Future studies comparing these *in vitro* models may identify cues essential for the full maturation and myelin sheet formation of SC OLCs.

Differential susceptibility to AMPAR-mediated excitotoxicity between FB and SC IMs

While SC OLCs appeared to be less active in proliferation and myelin formation, they were more resistant to AMPAR-mediated excitotoxicity than FB OLCs at IM stage. Importantly, we observed up-regulated GRIA2 expression in SC IMs. This suggests more contribution of edited GRIA2 into the AMPAR assembly forming Ca^{2+} impermeable AMPARs in SC IMs compared with FB IMs, which reduces the Ca^{2+} overloading and cellular stress during the exposure to KA. However, we failed to demonstrate a difference between SC IMs and FB IMs in $[Ca^{2+}]i$ elevations during a short-term exposure to KA. Our result indicates that even though proportionally high GRIA2-containing AMPARs in SC IMs may reduce long-term Ca^{2+} load and provide the partial protection to KA-induced excitotoxicity in SC IMs, $[Ca^{2+}]i$ homeostasis during a short-term activation of AMPAR was similarly maintained in both SC and FB IMs. Our finding warrants future studies in the detailed mechanisms underlying the differential vulnerability between FB and SC IMs, which will provide a significant insight to develop effective treatments for enhanced remyelination in the CNS circumstances where excitotoxic insults can occur due to high extracellular glutamate levels.

Differential expression of CNS region-specific TFs between FB and SC OLCs

Transcriptome analysis and semi-quantitative RT-PCR revealed that CNS region-specific TFs were retained in OPCs even after several passages *in vitro*. These results indicate that OPCs maintain regional identity in a cell-intrinsic and heritable manner as reported in NSCs (Kelly et al. 2009). CNS region-specific TFs play an essential role in the regionalization of the CNS cells particularly neurons. In the developing neurons, Hox TFs differentially expressed along the RC axis induce the region-specific expression of cell surface proteins essential for the formation of region-specific neuronal circuits and muscle innervation (Catela et al. 2016). Indeed, our transcriptome data identified many cell surface proteins differentially expressed between FB and SC OPCs, including those commonly regulated by Hox TFs in neurons during development, such as Epha5 and Epha7 (Alexander et al. 2009). This suggests active gene regulation by these TFs in OPCs and their involvement in the phenotypic differences between FB and SC OPCs. Semi-quantitative RT-PCR revealed that some of these TFs were detectable in IMs and MOs, although their expression was reduced compared with OPCs. The distinct gene regulation by these TFs in OPCs could remain even after the gene regulatory program for the oligodendrocytes differentiation is activated, and affect the phenotypes of IMs and MOs, such as the susceptibility to excitotoxicity and the robustness of myelin sheet formation. These lead to the hypothesis that CNS region-specific TFs play a role in shaping the region-specific phenotype of OLCs.

Clinical implications of the cell-intrinsic regional differences of OLCs along the RC axis

The regional differences of OLCs along the RC axis have significant clinical implications for the protection and repair of myelin in demyelinating diseases and conditions. Perinatal brain injury caused by hypoxia and ischemia severely damages premyelinating IMs in the

subcortical white matter resulting in periventricular leukomalacia (Volpe 2001). Although the unique vascular anatomy and the relatively late timing of myelination in the FB are responsible for the preferential vulnerability of subcortical white matter, our result that FB IMs were more susceptible to excitotoxicity than SC IMs suggests the involvement of OLC-intrinsic properties in the region-specific susceptibility to the perinatal brain injury. Moreover, the regional differences of OLCs along the RC axis may also affect myelin homeostasis and remyelination in the adult and aged CNS. A recent study demonstrated that the developmental heterogeneity of OLCs along the DV axis determines the remyelination responses to demyelination and age-associated functional decline of adult OPCs (Crawford et al. 2016). Our study extends this concept to the OPC heterogeneity along with the RC axis. Our data warrant future studies to determine whether regional heterogeneity in neonatal OPCs is inherited to adult OPCs and whether remyelination capacity of adult OPCs is affected by their region-specific characteristics. RNA sequencing together with cluster analyses will provide strong tools to approach this question as Marques et al. (2016) recently revealed molecular heterogeneity of adult OLCs. The knowledge obtained from such studies will provide novel target molecules to enhance remyelination in the adult and aged CNS. Moreover, recent studies have reported OPC generation from cells in non-CNS tissue, such as keratinocytes and fibroblasts through induced pluripotent stem cells (iPSCs) or a direct conversion, as sources of donor OPCs for transplantation therapies for the demyelinated CNS (Najm et al. 2013, Wang et al. 2013). Our results suggest that the regional identity of OPCs could be an important modulator of OPC properties such as their overall myelination efficiency. FB OPCs are superior in terms of proliferation and myelin sheet formation but more susceptible to excitotoxicity than SC OPCs. Thus, FB OPCs can be a better option for myelin repair if the excitotoxic microenvironment can be attenuated. It has been suggested that OPCs induced from human iPSCs by protocols using retinoic acid tends to have spinal or brainstem fate, while the recently reported retinoic acid-independent protocol favors telencephalic OPC production (Piao et al. 2015). Further studies will elucidate regional differences of OPC populations depending on the anatomical regions of origin and will suggest protocols for engineering the OPCs optimized for transplantation into demyelinating lesions under different pathological conditions.

Involves human subjects: No
If yes: Informed consent & ethics approval achieved:
=> if yes, please ensure that the info “Informed consent was achieved for all subjects, and the experiments were approved by the local ethics committee.” Is
included in the Methods.

ARRIVE guidelines have been followed:
Yes
=> if No or if it is a Review or Editorial, skip complete sentence => if Yes, insert “All experiments were conducted in compliance with the ARRIVE guidelines.
“ unless it is a Review or Editorial

Conflicts of interest: none

=> if ‘none’, insert “The authors have no conflict of interest to declare.”

=> otherwise insert info unless it is already included

Acknowledgments

We thank Ms. Elsie Lodde for proofreading and comments. This work was supported by Shriners Hospitals for Children Research Fellowship 84306 (M.H.), Shriners Hospitals for Children Grants 85400 (T.I.) and 85800 (A.I.), and National Institute of Health Grant NS025044 (D.P. and T.I.). We have no conflict of interest to declare.

Abbreviations

AM	acetoxymethyl ester
AMPA	α-amino-3-hydroxy-5-methyl-4-isoxazolepropionate
CNS	central nervous system
DAPI	4,6-diamidio-2-phenylindole
DV	dorsoventral
EdU	5-Ethynyl-2’-deoxyuridine
FB	forebrain
GO	gene ontology
HBSS	Ca^{2+} and Mg^{2+}-free Hank’s balanced salt solution
IM	immature oligodendrocyte
IFNγ	interferon-γ
iPSCs	induced pluripotent stem cells
KA	kainite
MBP	myelin basic protein
MO	mature oligodendrocyte
MTT	3-(4,5-Dimethylthiazol-2-yl)-2,5-diphenyltetrazolium bromide
NSC	neural stem cell
OLC	oligodendroglial lineage cell
OPC	oligodendroglial progenitor cell
$PDGF_{AA}$	platelet-derived growth factor A homodimer
PLP	myelin proteolipid protein
RC	rostrocaudal

SC	spinal cord
TFs	transcription factors

References

Aggarwal S, Yurlova L, Snaidero N et al. (2011) A size barrier limits protein diffusion at the cell surface to generate lipid-rich myelin-membrane sheets. Dev Cell, 21, 445–456. [PubMed: 21885353]

Akiyama T, Tominaga M, Takamori K, Carstens MI and Carstens E (2014) Roles of glutamate, substance P, and gastrin-releasing peptide as spinal neurotransmitters of histaminergic and nonhistaminergic itch. Pain, 155, 80–92. [PubMed: 24041961]

Alexander T, Nolte C and Krumlauf R (2009) Hox genes and segmentation of the hindbrain and axial skeleton. Annu Rev Cell Dev Biol, 25, 431–456. [PubMed: 19575673]

Bannerman P, Horiuchi M, Feldman D, Hahn A, Itoh A, See J, Jia ZP, Itoh T and Pleasure D (2007) GluR2-free alpha-amino-3-hydroxy-5-methyl-4-isoxazolepropionate receptors intensify demyelination in experimental autoimmune encephalomyelitis. Journal of neurochemistry, 102, 1064–1070. [PubMed: 17472701]

Barres BA and Raff MC (1994) Control of oligodendrocyte number in the developing rat optic nerve. Neuron, 12, 935–942. [PubMed: 8185952]

Bechler ME, Byrne L and Ffrench-Constant C (2015) CNS Myelin Sheath Lengths Are an Intrinsic Property of Oligodendrocytes. Current Biol, 18, 2411–2416.

Booth J, Nicolay DJ, Doucette JR and Nazarali AJ (2007) Hoxd1 is expressed by oligodendroglial cells and binds to a region of the human myelin oligodendrocyte glycoprotein promoter in vitro. Cellular and molecular neurobiology, 27, 641–650. [PubMed: 17554625]

Cai Z, Lin S, Pang Y and Rhodes PG (2004) Brain injury induced by intracerebral injection of interleukin-1beta and tumor necrosis factor-alpha in the neonatal rat. Pediatr Res, 56, 377–384. [PubMed: 15201401]

Carmon KS, Gong X, Lin Q, Thomas A and Liu Q (2011) R-spondins function as ligands of the orphan receptors LGR4 and LGR5 to regulate Wnt/beta-catenin signaling. Proc Natl Acad Sci U S A, 28, 11452–11457.

Carty ML, Wixey JA, Reinebrant HE, Gobe G, Colditz PB and Buller KM (2011) Ibuprofen inhibits neuroinflammation and attenuates white matter damage following hypoxia-ischemia in the immature rodent brain. Brain Res, 1402, 9–19. [PubMed: 21696706]

Catela C, Shin MM, Lee DH, Liu JP and Dasen JS (2016) Hox Proteins Coordinate Motor Neuron Differentiation and Connectivity Programs through Ret/Gfralpha Genes. Cell Rep, 14, 1901–1915. [PubMed: 26904955]

Chun SJ, Rasband MN, Sidman RL, Habib AA and Vartanian T (2003) Integrin-linked kinase is required for laminin-2-induced oligodendrocyte cell spreading and CNS myelination. The Journal of cell biology, 163, 397–408. [PubMed: 14581460]

Cohen SR and Guarnieri M (1976) Immunochemical measurement of myelin basic protein in developing rat brain: an index of myelin synthesis. Developmental biology, 49, 294–299. [PubMed: 1254097]

Crawford AH, Tripathi RB, Richardson WD and Franklin RJ (2016) Developmental Origin of Oligodendrocyte Lineage Cells Determines Response to Demyelination and Susceptibility to Age-Associated Functional Decline. Cell Rep 15, 761–773. [PubMed: 27149850]

Durand B, Fero ML, Roberts JM and Raff MC (1998) p27Kip1 alters the response of cells to mitogen and is part of a cell-intrinsic timer that arrests the cell cycle and initiates differentiation. Curr Biol, 8, 431–440. [PubMed: 9550698]

Fuccillo M, Rallu M, McMahon AP and Fishell G (2004) Temporal requirement for hedgehog signaling in ventral telencephalic patterning. Development, 131, 5031–5040. [PubMed: 15371303]

Fukai J, Yokote H, Yamanaka R, Arao T, Nishio K and Itakura T (2008) EphA4 promotes cell proliferation and migration through a novel EphA4-FGFR1 signaling pathway in the human glioma U251 cell line. Mol Cancer Ther, 7, 2768–2778. [PubMed: 18790757]

Groves AK, Barnett SC, Franklin RJ, Crang AJ, Mayer M, Blakemore WF and Noble M (1993) Repair of demyelinated lesions by transplantation of purified O-2A progenitor cells. Nature, 362, 453–455. [PubMed: 8464477]

Hall A, Giese NA and Richardson WD (1996) Spinal cord oligodendrocytes develop from ventrally derived progenitor cells that express PDGF alpha-receptors. Development, 122, 4085–4094. [PubMed: 9012528]

Hill RA, Patel KD, Medved J, Reiss AM and Nishiyama A (2013) NG2 cells in white matter but not gray matter proliferate in response to PDGF. J Neurosci, 33, 14558–14566. [PubMed: 24005306]

Horiuchi M, Itoh A, Pleasure D and Itoh T (2006) MEK-ERK signaling is involved in interferon-gamma-induced death of oligodendroglial progenitor cells. The Journal of biological chemistry, 281, 20095–20106. [PubMed: 16728393]

Horiuchi M, Itoh A, Pleasure D, Ozato K and Itoh T (2011) Cooperative contributions of interferon regulatory factor 1 (IRF1) and IRF8 to interferon-gamma-mediated cytotoxic effects on oligodendroglial progenitor cells. Journal of neuroinflammation, 8, 8. [PubMed: 21261980]

Horiuchi M, Lindsten T, Pleasure D and Itoh T (2010) Differing in vitro survival dependency of mouse and rat NG2+ oligodendroglial progenitor cells. J Neurosci Res, 88, 957–970. [PubMed: 19908280]

Horiuchi M, Maezawa I, Itoh A, Wakayama K, Jin LW, Itoh T and Decarli C (2012a) Amyloid beta1-42 oligomer inhibits myelin sheet formation in vitro. Neurobiology of aging, 33, 499–509. [PubMed: 20594620]

Horiuchi M, Wakayama K, Itoh A, Kawai K, Pleasure D, Ozato K and Itoh T (2012b) Interferon regulatory factor 8/interferon consensus sequence binding protein is a critical transcription factor for the physiological phenotype of microglia. Journal of neuroinflammation, 9, 227. [PubMed: 23020843]

Huang da W, Sherman BT and Lempicki RA (2009) Systematic and integrative analysis of large gene lists using DAVID bioinformatics resources. Nat Protoc, 4, 44–57. [PubMed: 19131956]

Itoh T, Beesley J, Itoh A, Cohen AS, Kavanaugh B, Coulter DA, Grinspan JB and Pleasure D (2002) AMPA glutamate receptor-mediated calcium signaling is transiently enhanced during development of oligodendrocytes. Journal of neurochemistry, 81, 390–402. [PubMed: 12064486]

Johns TG and Bernard CC (1999) The structure and function of myelin oligodendrocyte glycoprotein. Journal of neurochemistry, 72, 1–9. [PubMed: 9886048]

Johnston MV (2005) Excitotoxicity in perinatal brain injury. Brain Pathol, 15, 234–240. [PubMed: 16196390]

Kawahara Y, Ito K, Sun H, Kanazawa I and Kwak S (2003) Low editing efficiency of GluR2 mRNA is associated with a low relative abundance of ADAR2 mRNA in white matter of normal human brain. Eur J Neurosci, 18, 23–33. [PubMed: 12859334]

Kelly TK, Karsten SL, Geschwind DH and Kornblum HI (2009) Cell lineage and regional identity of cultured spinal cord neural stem cells and comparison to brain-derived neural stem cells. PloS one, 4, e4213. [PubMed: 19148290]

Kessaris N, Fogarty M, Iannarelli P, Grist M, Wegner M and Richardson WD (2006) Competing waves of oligodendrocytes in the forebrain and postnatal elimination of an embryonic lineage. Nature neuroscience, 9, 173–179. [PubMed: 16388308]

Levine J (2016) The reactions and role of NG2 glia in spinal cord injury. Brain Res, 1638, 199–208. [PubMed: 26232070]

Li C and Wong WH (2001) Model-based analysis of oligonucleotide arrays: expression index computation and outlier detection. Proc Natl Acad Sci U S A, 98, 31–36. [PubMed: 11134512]

Lin W, Kemper A, Dupree JL, Harding HP, Ron D and Popko B (2006) Interferon-gamma inhibits central nervous system remyelination through a process modulated by endoplasmic reticulum stress. Brain : a journal of neurology, 129, 1306–1318. [PubMed: 16504972]

Linneberg C, Harboe M and Laursen LS (2015) Axo-Glia Interaction Preceding CNS Myelination Is Regulated by Bidirectional Eph-Ephrin Signaling. ASN Neuro, 7.

Maier O, De Jonge J, Nomden A, Hoekstra D and Baron W (2009) Lovastatin induces the formation of abnormal myelin-like membrane sheets in primary oligodendrocytes. Glia, 57, 402–413. [PubMed: 18814266]

Marques S, Zeisel A, Codeluppi S et al. (2016) Oligodendrocyte heterogeneity in the mouse juvenile and adult central nervous system. Science, 352, 1326–1329. [PubMed: 27284195]

Mayer-Proschel M (2001) Isolation and generation of oligodendrocytes by immunopanning Current protocols in neuroscience / editorial board, Crawley Jacqueline N. … [et al.], **Chapter 3,** Unit 3 13.**Chapter 3,**

Miguez A, Ducret S, Di Meglio T et al. (2012) Opposing roles for Hoxa2 and Hoxb2 in hindbrain oligodendrocyte patterning. J Neurosci, 32, 17172–17185. [PubMed: 23197710]

Miller RH (2002) Regulation of oligodendrocyte development in the vertebrate CNS. Prog Neurobiol, 67, 451–467. [PubMed: 12385864]

Najm FJ, Lager AM, Zaremba A et al. (2013) Transcription factor-mediated reprogramming of fibroblasts to expandable, myelinogenic oligodendrocyte progenitor cells. Nature biotechnology, 31, 426–433.

Nicolay DJ, Doucette JR and Nazarali AJ (2004) Hoxb4 in oligodendrogenesis. Cellular and molecular neurobiology, 24, 357–366. [PubMed: 15206819]

Olsen IM and Ffrench-Constant C (2005) Dynamic regulation of integrin activation by intracellular and extracellular signals controls oligodendrocyte morphology. BMC Biol, 3, 25. [PubMed: 16283943]

Piao J, Major T, Auyeung G et al. (2015) Human embryonic stem cell-derived oligodendrocyte progenitors remyelinate the brain and rescue behavioral deficits following radiation. Cell stem cell, 16, 198–210. [PubMed: 25658373]

Rosenberg SS, Kelland EE, Tokar E, De la Torre AR and Chan JR (2008) The geometric and spatial constraints of the microenvironment induce oligodendrocyte differentiation. Proc Natl Acad Sci U S A, 105, 14662–14667. [PubMed: 18787118]

Schoenfeld R, Wong A, Silva J, Li M, Itoh A, Horiuchi M, Itoh T, Pleasure D and Cortopassi G (2010) Oligodendroglial differentiation induces mitochondrial genes and inhibition of mitochondrial function represses oligodendroglial differentiation. Mitochondrion, 10, 143–150. [PubMed: 20005986]

Sommer B, Kohler M, Sprengel R and Seeburg PH (1991) RNA editing in brain controls a determinant of ion flow in glutamate-gated channels. Cell, 67, 11–19. [PubMed: 1717158]

Tripathi RB, Clarke LE, Burzomato V, Kessaris N, Anderson PN, Attwell D and Richardson WD (2011) Dorsally and ventrally derived oligodendrocytes have similar electrical properties but myelinate preferred tracts. J Neurosci, 31, 6809–6819. [PubMed: 21543611]

van Heyningen P, Calver AR and Richardson WD (2001) Control of progenitor cell number by mitogen supply and demand. Curr Biol, 11, 232–241. [PubMed: 11250151]

Vigano F, Mobius W, Gotz M and Dimou L (2013) Transplantation reveals regional differences in oligodendrocyte differentiation in the adult brain. Nature neuroscience, 16, 1370–1372. [PubMed: 23995069]

Volpe JJ (2001) Neurobiology of periventricular leukomalacia in the premature infant. Pediatr Res, 50, 553–562. [PubMed: 11641446]

Wang S, Bates J, Li X et al. (2013) Human iPSC-derived oligodendrocyte progenitor cells can myelinate and rescue a mouse model of congenital hypomyelination. Cell stem cell, 12, 252–264. [PubMed: 23395447]

Weruaga-Prieto E, Eggli P and Celio MR (1996) Rat brain oligodendrocytes do not interact selectively with axons expressing different calcium-binding proteins. Glia, 16, 117–128. [PubMed: 8929899]

Xie D, Croaker GD, Li J and Song ZM (2016) Reduced cell proliferation and increased apoptosis in the hippocampal formation in a rat model of Hirschsprung's disease. Brain Res, 1642, 79–86. [PubMed: 27017960]

Young KM, Psachoulia K, Tripathi RB, Dunn SJ, Cossell L, Attwell D, Tohyama K and Richardson WD (2013) Oligodendrocyte dynamics in the healthy adult CNS: evidence for myelin remodeling. Neuron, 77, 873–885. [PubMed: 23473318]

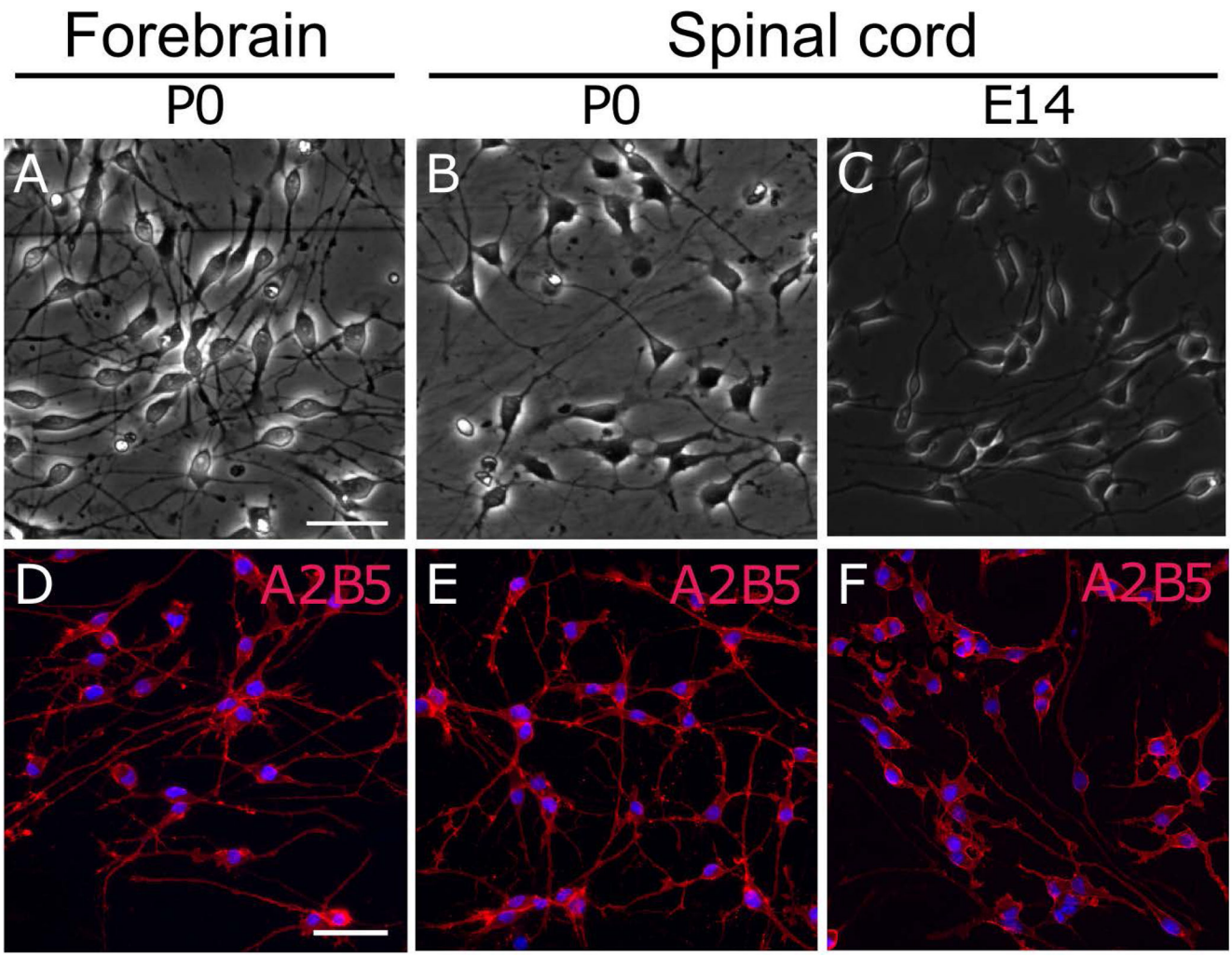

Figure 1.

Phase-contrast images (**A-C**) and A2B5 immunocytochemistry (**D-F**) of OPCs purified from P0 rat forebrains (**A, D**) and spinal cords (**B, E**), and those from E14 rat spinal cords. Cells were plated at x1 density. Scale bar: 50 μm.

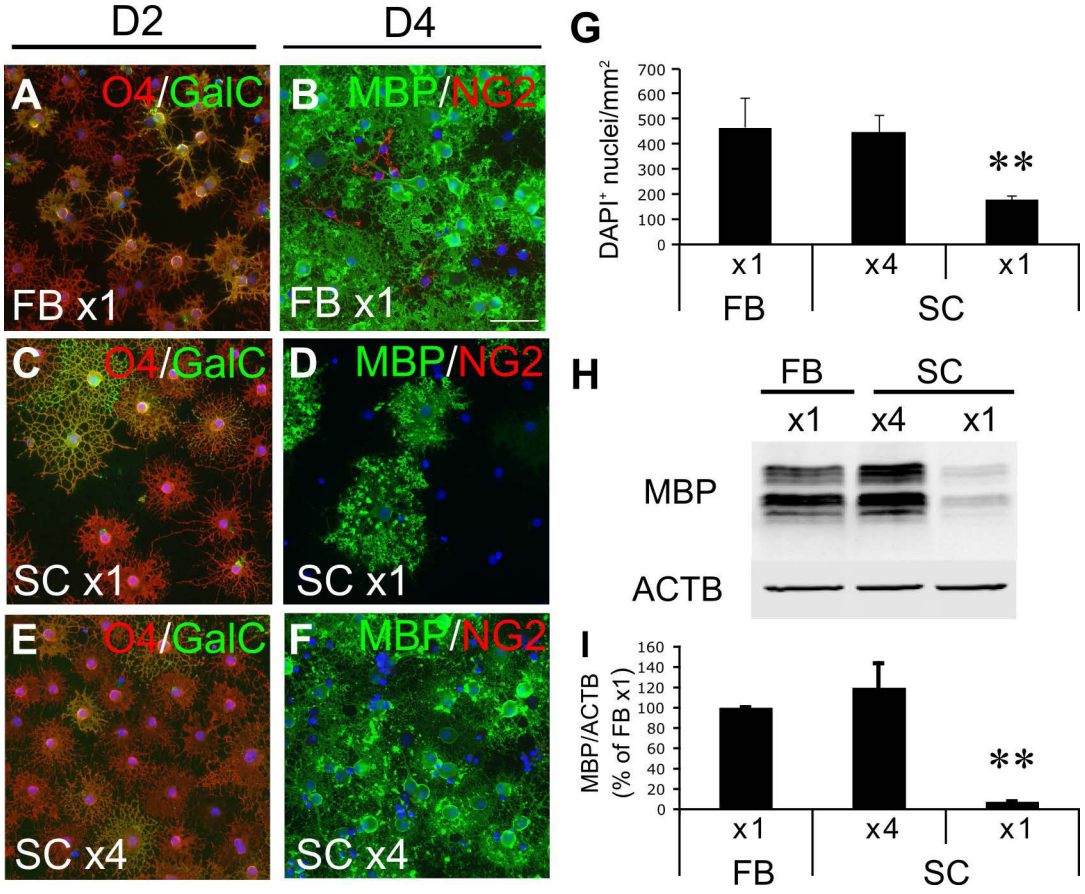

Figure 2.

In vitro differentiation of FB and SC OPCs. **A-F**, Immunocytochemistry of FB and SC OLCs at day 2 (D2; **A**,**C,E**) and day 4 (D4; **B,D,F**) in differentiation medium. Cells were stained for O4 antigen and galactocerebroside (GalC) at day 2 and for MBP and NG2 at day 4. Scale bar: 50 μm. **G,** Density of unfragmented DAPI+ nuclei in FB and SC cultures at day 4. **H-I**, A representative Western blot for MBP with protein samples from FB and SC OLC cultures at 4 days in differentiation medium (**H**) and the quantification of signal intensities from three independently conducted Western blots (**I**). ** indicates $p<0.01$ (n=3 independently prepared cultures/group, two-tailed ANOVA followed by Student-Newman-Keuls *post hoc* test). x1 and x4 indicate plating cell densities of 2.5×10^4 cells/cm^2 and 10^5 cells/cm^2, respectively.

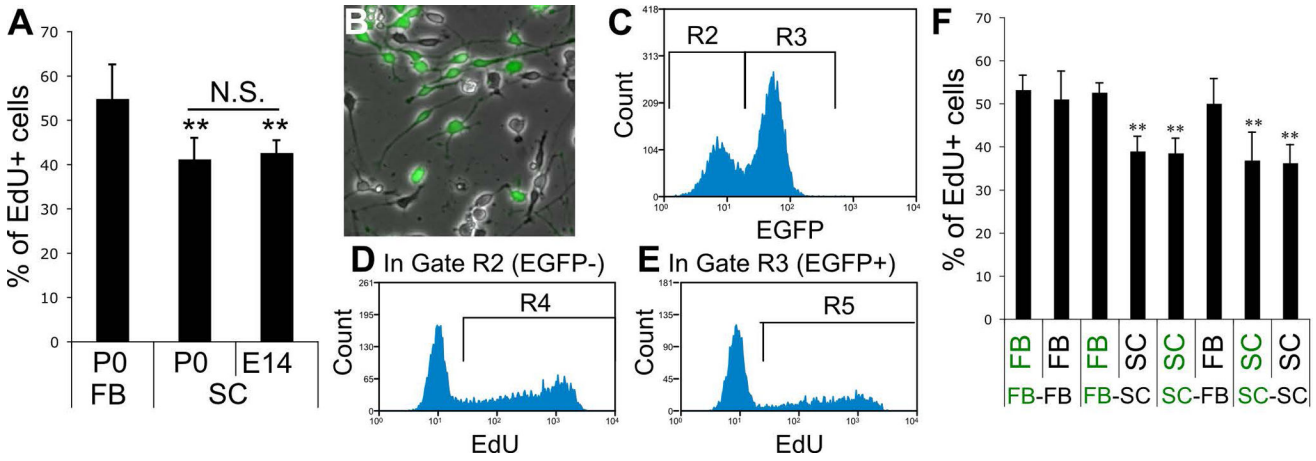

Figure 3.

A, EdU-incorporation assay of OPCs from P0 FB, and P0 and E14 SC. Cells were plated at x1 density. ** indicates $p<0.01$ ($n\geq9$ wells/group, two-tailed ANOVA followed by Student-Newman-Keuls *post hoc* test). **B-F**, OPC proliferation in FB-SC OPC co-cultures. **B**, Cells were mixed at 1:1 ratio and plated at x1 density. A representative phase contrast image of the co-culture of FB and SC OPCs. The green fluorescent overlay shows EGFP+ FB OPCs isolated from EGFP-transgenic rats. **C-E**, Representative histograms showing the gating strategy used for the quantification of EdU+ cells in EGFP− and EGFP+ cells in co-cultures. First, EGFP− and EGFP+ cells were gated by the gate R2 and R3, respectively (**C**). Then, number of EdU+ cells was counted by the gate R4 in the R2 (EGFP−) population (**D**) and by the gate R5 in the R3 (EGFP+) population (**E**). **F**, The percentage of EdU+ cells in EGFP− and EGFP+ cells in co-cultures of all four possible combinations. EGFP− and EGFP+ cells were indicated in black and green letters, respectively. ** indicates $p<0.01$ ($n=12$ wells/group, two-tailed ANOVA followed by Student-Newman-Keuls *post hoc* test).

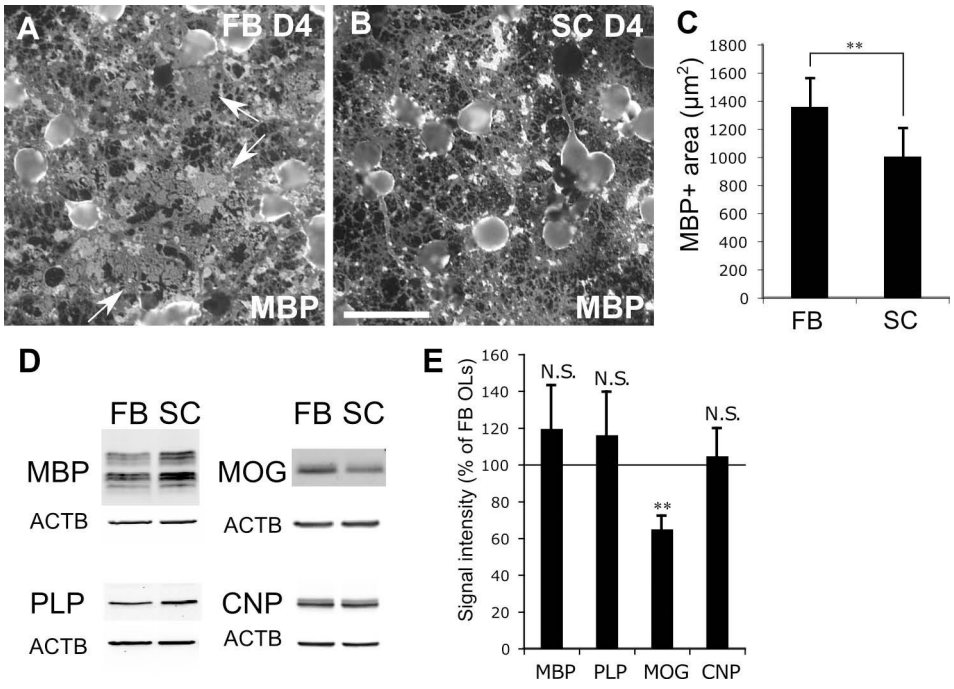

Figure 4.

A-C, *In vitro* myelin sheet formation by FB and SC OLCs. Representative immunocytochemistry for MBP of FB (**A**) and SC OLCs (**B**) at day 4 in differentiation medium. Arrows indicate typical MBP+ myelin sheets observed in FB MOs. Scale bar: 50 μm. **C** shows the quantification of area covered by MBP immunoreactivity in FB and SC OLC cultures. **D-E**, Expression of myelin proteins in differentiated FB and SC OLs in vitro. Representative Western blots for MBP, PLP, MOG and CNP (**D**), and the quantification (**E**). FB and SC cells were plated at x1 and x4 density, respectively. ** indicates $p<0.01$ (n=3 independently prepared cultures/group, Student's t-test).

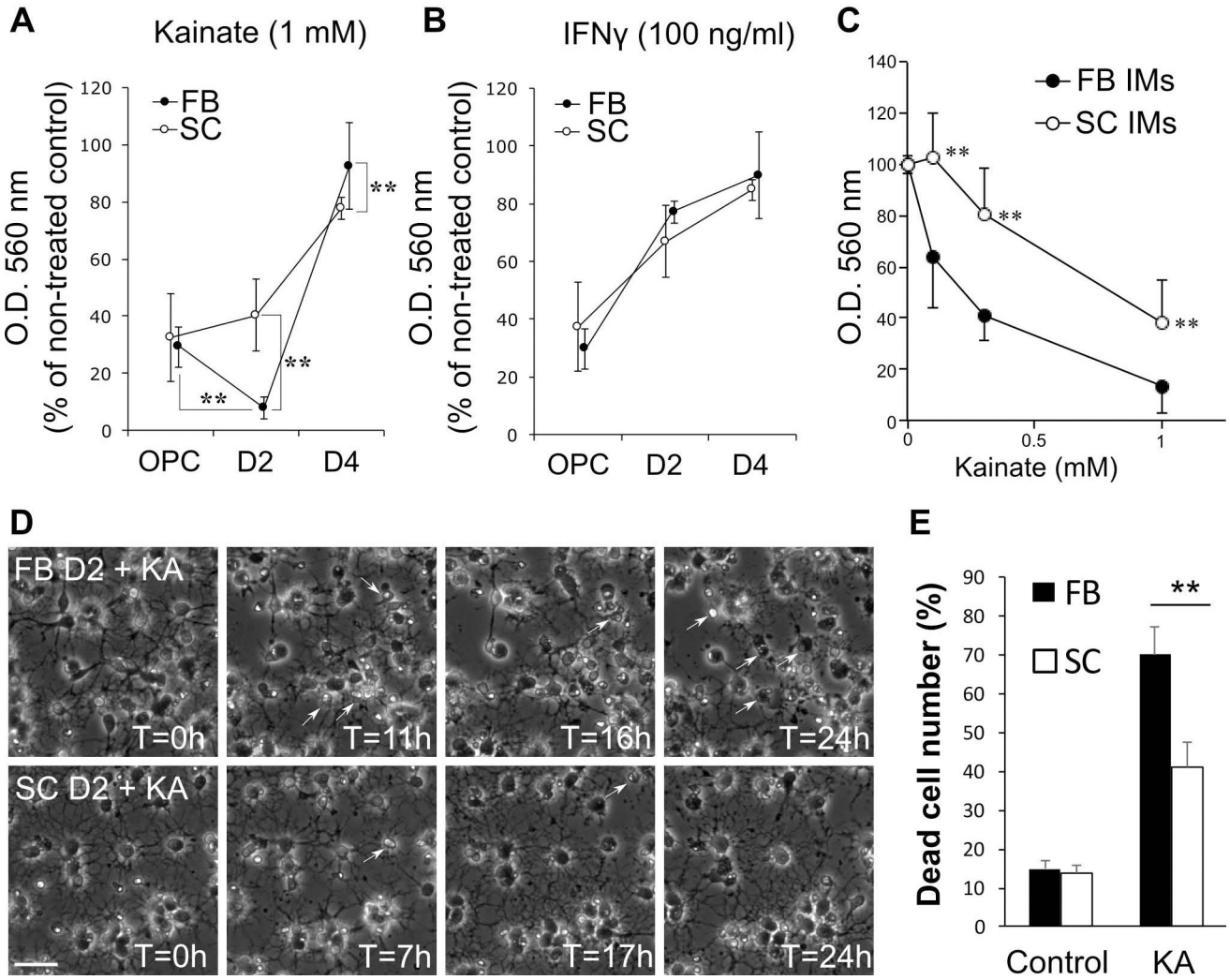

Figure 5.

A-B, Direct effects of KA-induced excitotoxicity and IFNγ-induced cytotoxicity on the viability of FB and SC OLCs at OPC, IM (D2), and MO (D4) stages. FB and SC cells were plated at x1 and x4 density, respectively. FB and SC cells at each stage were treated with KA (1 mM; A) or IFNγ (100 ng/ml; B) for 48 h and cell viability was measured by MTT assay. O. D. 560 nm values are presented as percentages of those of non-treated controls. ** indicate $p<0.01$ ($n\geq20$ wells/group, two-tailed ANOVA followed by Student-Newman-Keuls *post hoc* test). **C**, Dose-response effect of KA in excitotoxicity on forebrain (FB) and spinal (SC) IMs. Cells were treated with KA at 0.1, 0.3 and 1 mM for 48 h and cell viability was measured by MTT assay. ** indicates $p<0.01$ ($n=15$ wells/group, two-tailed ANOVA followed by Student-Newman-Keuls *post hoc* test). **D-E,** Time-lapse imaging of FB and SC IMs treated with KA (0.3 mM). **D,** Serial phase contrast images of FB (Top panels) and SC IMs (Bottom panels) at indicated time points after KA treatment at T=0. Arrows indicate dead cells detected based on morphological changes. **E,** Cumulative dead cell numbers in control and KA-treated FB and SC cultures for 24 h. ** indicates $p<0.01$ ($n=3$ independently

prepared cultures/group, two-tailed ANOVA followed by Student-Newman-Keuls *post hoc* test).

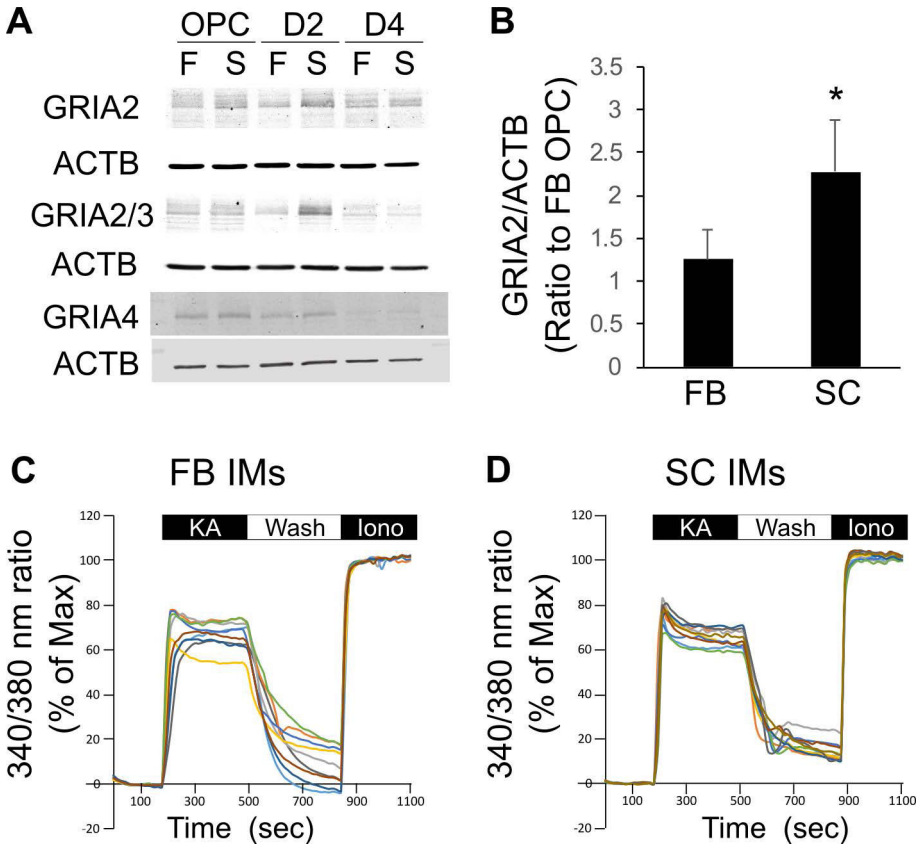

Figure 6.

A, Expression of AMPA-type glutamate receptor subunits, GRIA2, GRIA3, and GRIA4, was examined at OPC, D2, and D4 stages by Western blotting. FB and SC cells were plated at x1 and x4 density, respectively. **B**, Normalized signal intensities for GRIA2 on Western blots were compared between FB and SC IMs. * indicates $p<0.05$ (n=3 independent cultures/group, Student's t-test). **C-D**, Intracellular Ca^{2+} levels $[Ca^{2+}]_i$ in FB and SC IMs during the exposure to KA. Cells were exposed to KA (0.3 mM) from 3 min to 8 min for 5 min. After washing out KA, cells were exposed to ionomycin (Iono, 10 μM) to maximize $[Ca^{2+}]_i$. $[Ca^{2+}]_i$ was measured by 340 nm/380 nm fluorescent ratios of fura-2 AM, and indicated as percentages to the maximum $[Ca^{2+}]_i$ of each cell. FB and SC cells were plated at x1 and x4 density, respectively.

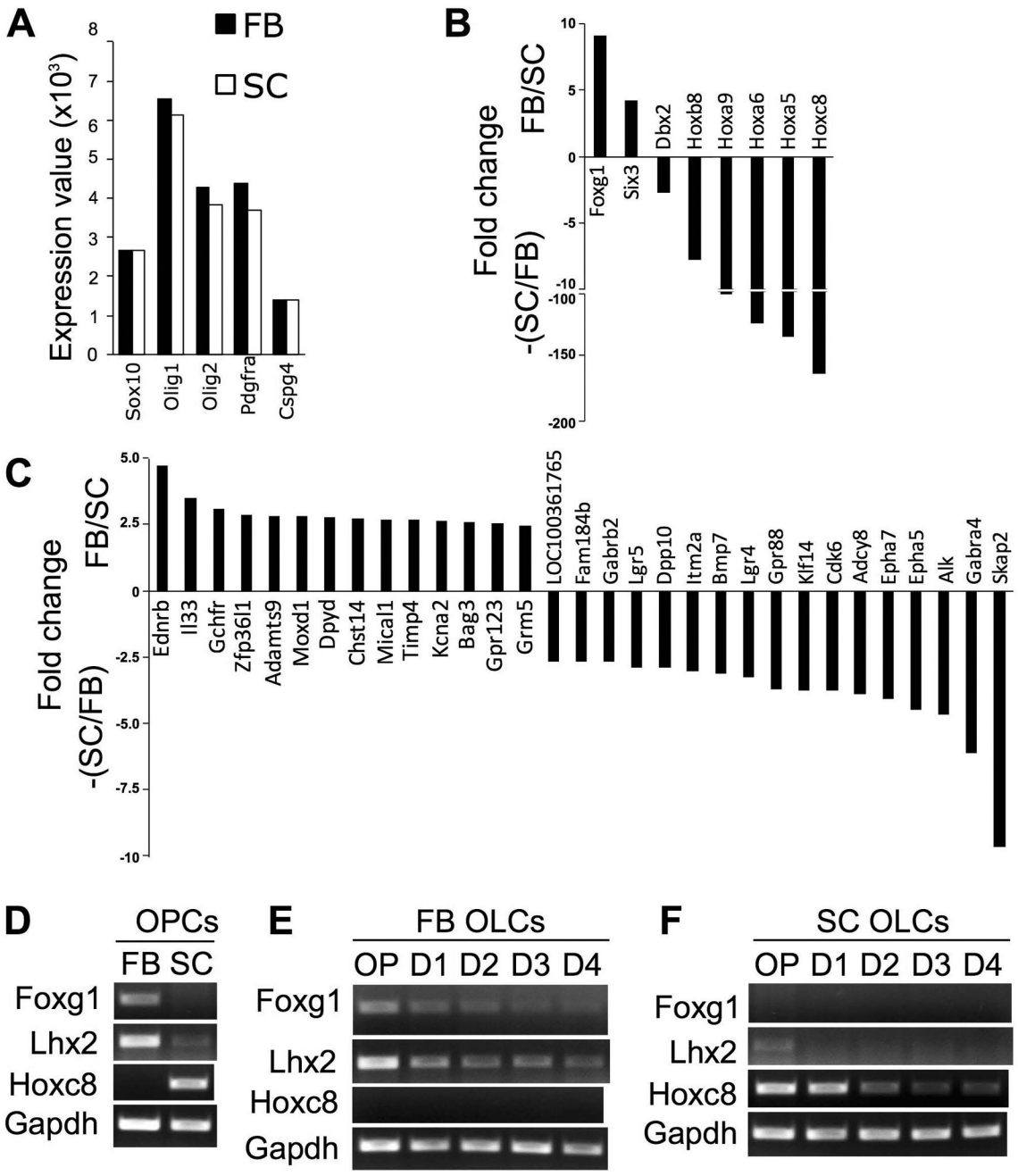

Figure 7.

A-B, Transcriptome analysis with Affymetrix GeneChip comparing gene expression profiles between FB and SC OPCs. **A**, Expression values of transcripts for OPC-specific genes, such as Sox10, Olig1/2, Pdgfra, and Cspg4, were not different between FB and SC OPCs. **B-C**, Genes differentially expressed between FB and SC OPCs. The fold differences of genes, which were expressed more than twice higher in FB OPCs compared with SC OPCs, are indicated as positive values (FB/SC), and the genes expressed at 2 or more times higher in SC OPCs than in FB OPCs are shown as negative values (-(SC/FB)). Genes encoding CNS region-specific transcription factors (TFs) (**B**) and those encoding non-TF proteins (**C**) are

separately shown. **D**, Semi-quantitative PCR examined the expression of CNS region-specific TFs, Foxg1, Lhx2, and Hoxc8. FB-specific TFs, Foxg1 and Lhx2, and SC-specific TF, Hoxc8, were expressed by FB and SC OPCs, respectively, in a mutually exclusive manner. **E-F**, Expression of these region-specific TFs was down-regulated as FB (**E**) and SC OPCs (**F**) differentiate into oligodendrocytes in vitro (D4 indicates 4 days in differentiation medium). Equal loading of samples was confirmed by the expression of Gapdh mRNA. FB and SC cells were plated at x1 and x4 density, respectively.

Table 1.

Immunocytochemical analysis of FB and SC OLCs in vitro

Stage	Marker	FB OLC (x1), n=5**	SC OLC (x4), n=5**
OPC	A2B5	99 ± 1%	99 ± 1%
	NG2	87 ± 4%	89 ± 2%
Day 2 in DM *	O4	96 ± 2%	93 ± 4%
	GalC	59 ± 13%	52 ± 7%
Day 4 in DM *	MBP	79 ± 6%	78 ± 7%

* DM: Differentiation medium

** n: number of cultures that were independently prepared

Table 2.

GO enrichment analysis comparing transcriptomes of FB and SC OPCs

GO cluster	FB OPC enriched			SC OPC enriched		
Homeobox	*Six3*			*Dbx2*	*Hoxa5*	*Hoxb8*
				Hoxa9	*Hoxc8*	
GABAergic synapse				*Adcy8*	*Gabra4*	*Gabrb2*
Transmembrane	*Ednrb*	*Grm5*	*Kcna2*	*Epha5*	*Epha7*	*Gpr88*
	Gpr123			*Adcy8*	*Alk*	*Dpp10*
				Gabra4	*Gabrb2*	*Itm2a*
				Lgr5	*Lgr4*	
Protein tyrosine kinase activity				*Epha5*	*Epha7*	*Alk*
Ion channel	*Kcna2*			*Gabra4*	*Gabrb2*	
G-protein coupled receptor	*Ednrb*	*Grm5*	*Gpr123*	*Gpr88*	*Lgr5*	*Lgr4*